ELSEVIER Superlattices and Microstructures 33 (2003) 397–403

Superlattices and Microstructures

www.elsevier.com/locate/jnlabr/yspmi

A quantum electromechanical device: the electromechanical single-electron pillar

Robert H. Blick[a,*], Dominik V. Scheible[b]

[a] *Electrical and Computer Engineering, University of Wisconsin-Madison, 1415 Engineering Drive, Madison, WI-53706, USA*

[b] *Center for NanoScience, Ludwig-Maximilians-Universität, Geschwister-Scholl-Platz 1, 80539 Munich, Germany*

Accepted 20 February 2004

Abstract

A new nanoelectromechanical device is introduced, useful for quantum electromechanics. The focus will be on single-electron transistors with a mechanical degree of freedom. The technical approach as well as the experimental realization of a new *vertical* mechanical single-electron tunneling device are discussed. This transistor is fabricated in a semiconductor material, forming a nanopillar between source and drain contacts. This concept can readily be transferred to large scale fabrication, being of importance for building integrated sensors and amplifier stages for quantum electromechanical circuits. Operation of the device at room temperature in the frequency range of 350–400 MHz is presented. A straightforward theoretical model of device operation is given.

PACS: 73.23.-b; 87.80.Mj

Keywords: NEMS; Single-electron tunneling; Quantum electromechanics

The integration of a mechanical degree of freedom into nanostructures now allows one to lay out circuits for nanoelectromechanical systems (NEMS) promising a wide range of applications in sensor and communication electronics [1, 2]. Mechanical resonators manufactured with nanometer dimensions oscillate at radio frequencies [3] and are

* Corresponding author.
E-mail address: blick@engr.wisc.edu (R.H. Blick).

0749-6036/$ - see front matter © 2004 Elsevier Ltd. All rights reserved.
doi:10.1016/j.spmi.2004.02.021

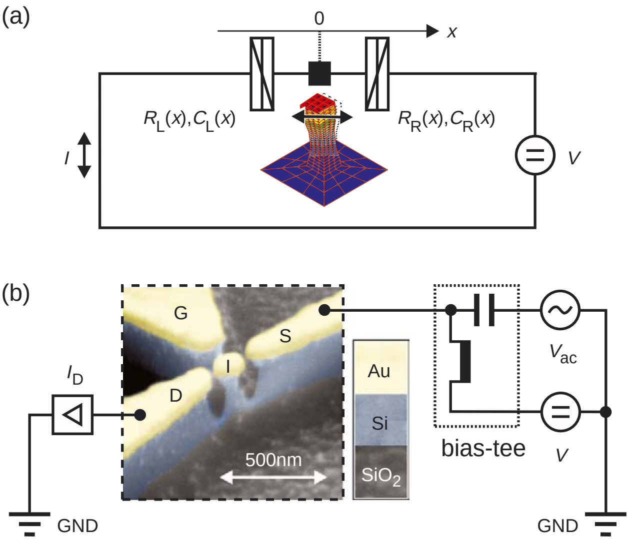

Fig. 1. (a) The circuit diagram for the electromechanical single-electron transistors (emSETs): as for conventional SETs, the metallic island in the center is connected to the leads via a parallel combination of tunneling resistance and lead/transistor capacitance. In addition, diagonal lines with different orientations have been added. These indicate the 'mechanical' cross-coupling of the barriers $R_{L/R}(x)$, $C_{L/R}(x)$; i.e. once electrons tunnel through the left barrier, tunneling through the right barrier is suppressed. As an inset, the finite element simulation of the island at the end of an oscillating pillar is shown. The ground mode is found to be at $f_0 = 367$ MHz. (b) A high-resolution scanning electron beam picture and the experimental set-up. At the source contact (S) an AC signal is applied, V_{AC}, with a superimposed DC bias, V. The net current, I_D, is detected at the drain contact (D) with a current amplifier.

entering the GHz domain [4]. As regards control of non-linear dynamics [5, 6] and dissipation [7] of NEMS at radio frequencies, tremendous progress has been achieved. Moreover, NEMS promise experimental insight into quantum aspects of mechanical systems. The level of device sensitivity achievable already supports terming the field 'quantum electromechanics' (QEM) [8].

Here, we want to give a specific example of a circuit already implemented. The approach promises to satisfy industrial demand for highly integrated and robust electromechanical circuits and the research driven quest for quantum limited displacement detection. The concept basically relies on combining nanomechanical resonators with single-electron transistors (SET). In the first versions of this circuit we combined cantilevers and fabricated SETs on the tips of these [9, 10], forming a so-called electromechanical SET or emSET. To achieve this we began with traditional NEMS fabrication by using optical and electron beam lithography of layered silicon substrates incorporating a sacrificial layer. The very first success was in proving that electron tunneling can be mechanically chopped at radio frequencies in the range of 10–100 MHz [9]. This shuttling of electrons by a mechanical switch can be represented conceptually as in the circuit diagram of Fig. 1(a). As known from work on single-electron tunneling, the barriers of the electron island to drain and source are represented by a parallel combination of the tunneling resistance R

and the junction capacitance C. However, since we are dealing with mechanically flexible tunneling barriers the notation is slightly different. This is indicated by the diagonal lines through the R/C boxes. These two lines are not parallel, relating to the fact that once the left (source) junction is tuned mechanically into the open state, the right (drain) junction will be opaque. In the following, we will demonstrate a new concept for manufacturing and operating a silicon nanopillar switching single-electron flow, similar to an electron shuttle, at 0.4 GHz. The main difference from the 'classical' version is found in the vertical and thus highly integrated approach.

The nanomechanical switch operates in the radio-frequency range. The device is realized in industry standard silicon material (silicon-on-insulator, SOI) with a metallic top layer. In Fig. 1(b) an electron beam micrograph of the readily fabricated device is shown: the underlying silicon dioxide is the substrate base, supporting the mechanical pendulum (I = island) in the center between the drain (D) and source (S). The island can be thought of as a nanopillar with a solid silicon single-crystalline base and a gold cap layer. The switch is controlled by biasing the source and drain and/or the controlling gate voltage (G). This island serves as the charge shuttle. As seen in the finite element simulation [Fig. 1(a)], we find a mechanical resonance frequency of the device of the order of 367 MHz [11]. This frequency depends on the pillar height, as well as on the material constants and the metallic top layer mass. Excitation of the nanomechanical resonator is most efficiently provided by AC and DC biasing through the contacts D and S. The resulting drain current flow I_D is then determined by a current/voltage converter.

Of prime importance for a device functioning as a switch or signal filter is the fact that its throughput resistance is drastically enhanced, since only one contact (D or S) is open during a half-cycle of operation: once the island is biased, a certain number of electrons N will flow onto the island (depending on the island's electrostatic potential) and jump off the island only when the other contact comes into reach during the second half-cycle of the switch revolution. In contrast to the earlier realizations of the emSET this novel vertical emSET (VemSET) allows for straightforward integration in any silicon based circuit requiring signal switching and/or filtering. This is achieved with a single lithographic process and a single etching step, thus reducing the processing complexity and time drastically.

For excitation we employ an AC voltage at the source contact. Moreover, application of an AC signal allows one to excite the nanopillar resonantly in one of its eigenmodes. Gradually accumulating charge on the island results in a resonant Coulomb force (RCF) within the AC source–drain field. The basic concept underlying the device is the excitation of mechanical oscillation via the excess charge on the island. Hitherto employed excitation mechanisms, such as magnetomotive driving, are not applicable for mass-production devices, due to the high magnetic field which is required ($B \sim$ 1–10 T). In addition, our device can be operated without cryogenic cooling and achieves accurate and well reproducible operation in the temperature range of 77–300 K.

During this deflection, the shuttle exchanges charge carriers with the gate: N electrons tunnel off the island and M electrons tunnel from the gate to the shuttle. The respective amounts N and M are determined by the instantaneous electrical bias [see Fig. 2(c)]. The detected current I_D is the net number of transferred electrons n times the shuttle

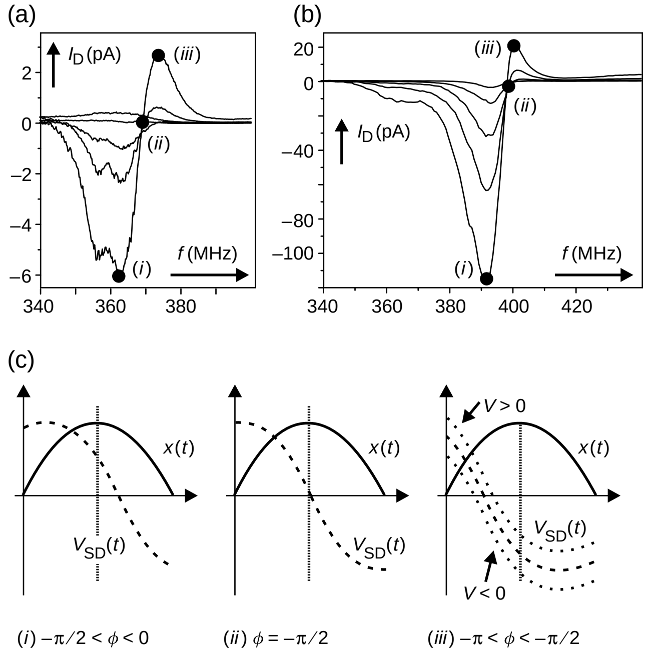

Fig. 2. (a) and (b): spectral drain current I_D versus source frequency f for two nanopillar devices. In (a) power P ranges from 0 to +10 dBm and for (b) from +2 to +8 dBm. The resonance frequencies are $f(a)_0 = 369$ MHz and $f(b)_0 = 399$ MHz, respectively. (c) Phase relations of the pillar deflection and source–drain bias. For a driven harmonic oscillator the phase lag ϕ_h varies from 0 to $-\pi$ and assumes $-\pi/2$ for resonance ($f = f_h$). In this case (ii) maximum island deflection is found at the moment when the voltage bias vanishes, and hence no net current flows. (i) and (iii) show the cases $f < f_h$ and $f > f_h$ respectively.

frequency f:

$$I_D = gef(N - M) = gefn \tag{1}$$

where e is the electronic charge and g accounts for a statistical limitation for the case where deflection is not sufficient for charge transport in each cycle. For the excitation via the resonant Coulomb force it is necessary that the shuttle sustains a certain excess charge during oscillation. This is ensured by a mechanical asymmetry which strongly favors one tunneling barrier at which the shuttle is reset to the same charge state each cycle. We assume m electrons present on the shuttle for the time period when both tunneling barriers are closed. For stable operation the relation $(N - M) = n < m$ must hold. The RCF is then calculated via

$$F_{\mathrm{RCF}}(t) = me\frac{\hat{V}_{\mathrm{AC}}\sin(2\pi f t)}{d_{\mathrm{SD}}} \tag{2}$$

with $\hat{V}_{\mathrm{AC}}$ being the AC amplitude and d_{SD} the source–drain distance. Via a finite element simulation we can estimate the gate island capacitance to be $C_{\mathrm{SI}} = 10$ aF. This results in a maximum excess charge $m = 24$ electrons, causing, in turn, a force of 7 pN at an incident

AC power of $P = +5$ dBm. Important for the current frequency behavior is the phase relation of the mechanical motion and the electrical AC bias. In the case of a harmonic oscillator (HO), the driven resonator follows the applied force with a phase lag of

$$\phi_h(f) = \arctan \frac{\Gamma f}{f_h^2 - f^2} \tag{3}$$

with the resonance frequency f_h. For excitation of a mechanical eigenmode h of the nanopillar the phase lag equals $\phi_h = -\pi/2$, i.e. maximum deflection occurs when $N = M$. For an ideal system, we accordingly expect a zero net current $I_D = 0$ for $f = f_h$. Above and below the resonance frequency f_h, the phase lag approaches $-\pi$ and zero respectively. Depending on the sign of the excess charge m, we find either a positive current for $f > f_h$ and a negative current for lower frequencies or vice versa.

We have carried out basic measurements of the current frequency response for a couple of devices showing similar behavior at slightly different eigenfrequencies f_0. This variation is explained by the different heights and waistlines of the pillar. Via a finite element simulation [11] both the absolute resonance frequencies and variations were well reproduced. The current traces I_D for a set of AC powers P are plotted in Fig. 2(a) and (b). Highest current amplitudes correspond to a transported net amount of electrons $n < 2$ following Eq. (1), which satisfies well the condition $n < m$. For the two samples the negative and positive peak currents differ by factors of 2 and 5, respectively. Mechanical asymmetry and inhomogeneity of the effective electric field destroy the phase relation of an ideal HO, and hence cause the asymmetric peaks.

The mechanism of RCF can be verified in the present set-up via a superposition of a DC bias V onto the AC voltage V_{AC}. This is accomplished by an inserted bias-tee; see Fig. 1(b). As long as the DC bias is small compared to the AC amplitude $\hat{V}_{\mathrm{AC}}$, the main influence is the phase shift between the deflection point and the effective drain/source bias [see Fig. 2(c)]. As a result, we accomplished switching between forward and reverse current peaks (i) and (iii), as well as zero current (ii). In Fig. 3(a) we show the spectral current for a set of selected DC bias voltages ranging from -70 to $+40$ mV. It is important to note that the observed behavior not only supports RCF, but also demonstrates the tunability of this mechanical device. This will turn out to be important for rectification of high-frequency AC signals. A summary of all traces at the lower and upper peak frequencies $f_0^{\pm}$ reveals that the peaks are not only detuned, but also can give a reverse current response. As Fig. 3(b) shows, this is achieved for a high DC bias exceeding 40 mV. In addition to the detuning, a regular step-like structure is observed in both peaks when the DC bias is ramped. The separation of the steps ($\sim$23 mV) corresponds to the island/gate capacitance; however, the total island capacitance for room temperature operation should only be $e^2/k_{\mathrm{B}}T \approx 3$ aF. Hence, we attribute the steps to a gradual change of the oscillatory mode rather than Coulomb blockade effects. Nevertheless, this indicates that observation of Coulomb blockade effects with semiconductor charge shuttles is now within reach.

We have shown how to realize semiconductor charge shuttles in a new and straightforward manner which is both applicable for industrial application as well as of interest for quantum electromechanics. The measurements not only prove our earlier results obtained on conventional electromechanical single-electron transistors, but additionally

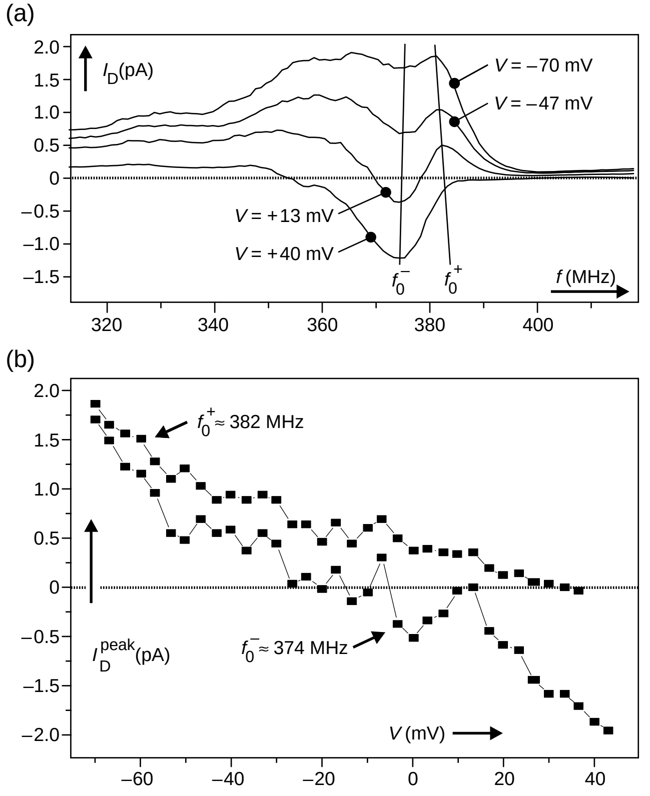

Fig. 3. (a) Tuning of the current resonance by a superimposed DC bias V. Both negative and positive current response are entirely detuned by the respective bias. This is a further test of the excitation of the electron shuttle via the resonant Coulomb force (RCF). (b) Negative (lower trace) and positive (upper one) peak currents I_D^{peak} versus DC bias V. The traces represent a section of the whole set of current spectra at frequencies $f_0^- \sim 374$ MHz and $f_0^+ \sim 382$ MHz.

reveal how to effectively control NEMS. The next steps to be taken will focus on realizing combined AC/DC self-excited shuttles in phase-locked circuits.

Acknowledgements

RHB would like to thank A. Erbe, D.R. König, Ch. Weiss, and W. Zwerger for discussion and the Deutsche-Forschungsgemeinschaft (DFG) for support through grant Bl-487/1.

References

[1] M.L. Roukes, Phys. World 14 (2001) 25.
[2] C.T.-C. Nguyen, IEEE Trans. Microwave Theory Tech. 47 (1999) 1486.

[3] R.H. Blick, A. Erbe, L. Pescini, A. Kraus, D.V. Scheible, F.W. Beil, E.M. Hoehberger, A. Hoerner, J. Kirschbaum, H. Lorenz, J.P. Kotthaus, J. Phys.: Cond. Mat. 14 (2002) R905.
[4] X.M.H. Huang, C.A. Zorman, M. Mehregany, M.L. Roukes, Nature (London) 421 (2003) 496.
[5] D.V. Scheible, A. Erbe, G. Corso, R.H. Blick, Appl. Phys. Lett. 81 (2002) 1884.
[6] D.V. Scheible, A. Erbe, R.H. Blick, Appl. Phys. Lett. 82 (2003) 3333.
[7] F.W. Beil, R.H. Blick, A. Wixforth, W. Wegscheider, M. Bichler, D. Schuh, Phys. Rev. Lett. (2004) (submitted for publication).
[8] M. Blencowe, Phys. Rep. (2003) (submitted for publication).
[9] A. Erbe, R.H. Blick, A. Tilke, A. Kriele, J.P. Kotthaus, Appl. Phys. Lett. 73 (1998) 3751.
[10] A. Erbe, Ch. Weiss, W. Zwerger, R.H. Blick, Phys. Rev. Lett. 87 (2001) 096106.
[11] SOLVIA, Finite element system for solving mechanical eigenmodes (ver. 99.0).